https://doi.org/10.5194/egusphere-2025-5131
Preprint. Discussion started: 18 November 2025

Combined effects of low temperature and low light intensity on elemental content and macromolecules of coccolithophores

Jinlong Shang[1,§], Wenting Ke[2,§], Yinrui Wang[3,§], Junqin Cai[3], Yan Chen[3], Xi Liu[3], Yonghe Han[3], Hong Zhang[3], Kui Xu[4], Yong Zhang[3]

[1]College of Life Science and Xinjiang Key Laboratory of Special Species Conservation and Regulatory Biology, Xinjiang Normal University, Urumqi 830054, Xinjiang, China
[2]School of Primary Education, Wuhan City Polytechnic, Wuhan 430065, China
[3]College of Environmental and Resource Sciences, College of Carbon Neutral Modem Industry, Fujian Key Laboratory of Pollution Control and Resource Recycling, Fujian Normal University, Fuzhou 350117, China
[4]Hubei Key Laboratory of Edible Wild Plants Conservation and Utilization, Hubei Engineering Research Center of Special Wild Vegetables Breeding and Comprehensive Utilization Technology, College of Life Sciences, Hubei Normal University, Huangshi 435002, China

Running head: Temperature and light on coccolithophores

Correspondence to: Wenting Ke (kewenting@whcp.edu.cn); Yong Zhang (yongzhang@fjnu.edu.cn)
[§]These authors contributed equally to this work.

Keywords: coccolithophores, elemental content, low temperature, low light intensity, macromolecules

https://doi.org/10.5194/egusphere-2025-5131
Preprint. Discussion started: 18 November 2025

Abstract

The calcifying coccolithophores *Gephyrocapsa oceanica* and *Emiliania huxleyi* can grow preferentially in deep waters (150–200 m), however, their physiological and biochemical strategies for acclimating to the combined constraints of low temperature and low irradiance remain unclear. In this study, we subjected three coccolithophore strains (*G. oceanica* NIES–1318, *E. huxleyi* PML B92/11 and RCC1266) to low temperature (9°C) and low light intensity (15 µmol photons m^{-2} s^{-1}), and compared their growth rates, particulate inorganic carbon (PIC), particulate organic carbon (POC), nitrogen (PON) and phosphorus (POP) contents, as well as carbohydrate and lipid levels, with those under standard cultivation (21°C, 150 µmol photons m^{-2} s^{-1}). The results revealed that low temperature and low light intensity acted synergistically to decrease growth rate, POC contents and the POC : PON and POC : POP ratios, whereas did not significantly affect POP content in any of the strains. While increased light intensity enhanced PIC and PON contents at high temperature, it reduced them at low temperature. Low light intensity was identified as the primary factor leading to reduced carbohydrate and lipid level. Collectively, these findings indicate that to acclimate to low–temperature and low–light conditions, coccolithophores prioritized reducing the metabolic cost of carbohydrate and lipid biosynthesis, thereby allocating more resources to phosphorus metabolism–a physiological adjustment that can significantly influence biogeochemical cycles in the deep ocean.

https://doi.org/10.5194/egusphere-2025-5131
Preprint. Discussion started: 18 November 2025

1 Introduction

Coccolithophores are a type of unicellular eukaryotic calcifying algae and widely distributed throughout the global oceans (Hernández–Almeida et al., 2020). They fix CO_2 into organic carbon via photosynthesis, and produce $CaCO_3$ (coccoliths) through calcification which releases CO_2 into the surrounding environment, enhances particle settling and facilitates the burial of carbon at depths (Skeffington et al., 2022). Hence, coccolithophores make significant contributions to biological organic carbon pump and the carbonate counter pump (Li et al., 2024). Their comparatively low requirements of nitrogen and phosphorus enable dominance in oligotrophic provinces, e.g., sectors of the North Atlantic and Southern Ocean (Malinverno et al., 2003; Rigual Hernández et al., 2020), and bloom–forming species such as *Gephyrocapsa oceanica* and *Emiliania huxleyi* can restructure local ecosystem function (Poulton et al., 2014). Notably, coccolithophores are capable of carrying out photosynthesis near or below the base of the euphotic zone (150–200 m)–e.g., in the north–eastern Caribbean and South Pacific Gyre with low temperature (< 12ºC) and low irradiance level (< 20 µmol photons m^{-2} s^{-1}), and occupying resource niches that contribute to the stability of deep–water primary production (Jordan and Winter, 2000; Beaufort et al., 2007). Despite their ecological prominence, to our knowledge, the physiological and biochemical strategies enabling coccolithophores to tolerate the simultaneous constraints of low–temperature and low–irradiance conditions prevalent in deeper waters remain poorly resolved.

Prior work has identified several low–temperature acclimate strategies of coccolithophores. Under decreasing temperature conditions, *G. oceanica* increased cellular particulate organic carbon (POC) and nitrogen (PON) content, and decreased cellular chlorophyll *a* and alkenone contents (Torres–Romero et al., 2024). The biochemical mechanisms for high POC and PON contents in low temperature condition

https://doi.org/10.5194/egusphere-2025-5131
Preprint. Discussion started: 18 November 2025

could be that coccolithophores can decrease enzymatic turnover rates or productivity through decreasing the activity of thermally sensitive enzymes, whereas increase the abundances of these enzymes to compensate partly for the lower efficiency (Petrou et al., 2016). For example, the abundances of carboxylating enzyme Ribulose–1,5–bisphosphate carboxylase/oxygenase (Rubisco) were 2–3 folds higher in phytoplankton collected from the Southern Ocean than from the temperate oceans (Sage, 2002; Young et al., 2015). In addition, the coccolithophore *G. oceanica* and *E. huxleyi* can produce unsaturated long chain alkenones (C37–C39) (Conte et al., 1998), and increase the unsaturation of alkenones to regulate the microstructure of membrane lipids, which enhances the stability of the membrane under low temperature conditions (Conte et al., 2006). These studies elucidate the mechanisms of coccolithophore adaptation to low temperatures in physiological and biochemical levels (Dedman et al., 2023; Torres–Romero et al., 2024). However, there is limited work studying the biogeochemical effects of coccolithophores under low temperature conditions, such as the response of carbon (C) : nitrogen (N) : phosphorus (P) ratios and their impacts on deep–sea ecosystems.

Coccolithophores have unique features in their response to low light conditions. Recently, Shen et al. (2025) purified a photosystem I (PSI)–fucoxanthin chlorophyll a/c–binding protein (PSI-FCPI) supercomplex from the coccolithophore *Emiliania huxleyi* (Eh). This monomeric supercomplex contains 12 PSI core subunits, a specific lumenal linker protein (EhLP), and 38 peripheral Eh–FCPI antennae, which constitutes the largest PS–antenna supercomplex known so far. High levels of chlorophyll c and fucoxanthin allow fast kinetics and the absorption of blue-green light, suitable for the deep ocean–dwelling coccolithophore (Shen et al., 2025). In low light intensity, coccolithophore increases the functional absorption cross–section, quantum efficiency,

https://doi.org/10.5194/egusphere-2025-5131
Preprint. Discussion started: 18 November 2025

Chl *a* and carotenoid contents to increase the absorption of light (Zhang and Gao, 2021). Furthermore, it is hypothesized that the refractive index of coccoliths (approximately 1.65) is higher than that of seawater (approximately 1.33) (Horváth and Varjú, 2004). This structure acts as a micro–lens, focusing incoming blue–green light onto the chloroplasts and increasing the local light intensity (Young et al., 1999). This light–concentrating effect can enhance photosynthetic efficiency, particularly in the deep ocean (Triccas et al., 2025). However, to our knowledge, a limited number of studies have examined the variation in physiological and biochemical characteristics across different coccolithophore strains in response to low light intensity.

While most research on the combined influences of temperature and light intensity on coccolithophores has focused on range of 10–24°C and 60–480 µmol photons m^{-2} s^{-1} (Feng et al., 2008; Jin et al., 2019; Zhang et al., 2020), few have examined the extreme conditions of low–temperature and low–light intensity simultaneously. In this study, we exposed three coccolithophore strains to low temperature (9°C) and low light (15 µmol photons m^{-2} s^{-1}) conditions, comparing their growth rates, particulate organic carbon (POC), nitrogen (PON) and phosphorus (POP), carbohydrate and lipid contents to those under standard cultivation (21°C and 150 µmol photons m^{-2} s^{-1}). This study aims to investigate the physiological and biochemical responses of coccolithophores to low–temperature and low–light intensity, and tries to assess the consequences for the deep–sea carbon cycle.

2 Materials and methods

2.1 Strains and culture conditions

Gephyrocapsa oceanica strain NIES–1318 was originally isolated from the coastal water around Japan, and obtained from the center for collections of marine bacteria and

https://doi.org/10.5194/egusphere-2025-5131
Preprint. Discussion started: 18 November 2025

algae, Xiamen University, China. *Emiliania huxleyi* strain PML B92/11 was isolated from the coastal waters off Bergen, Norway, and obtained from the Plymouth algal culture collection, UK. *Emiliania huxleyi* strain RCC1266 was isolated from shelf waters around Ireland, and obtained from the Roscoff algal culture collection, France (Jin et al., 2019; Zhang et al., 2021).

In the control treatment, cells were maintained in 150 µmol photons m^{-2} s^{-1} of photosynthetically active radiation (PAR, high light intensity, HL) (measured using a PAR Detector, PMA 2132 from solar light company) under a 16 h: 8 h light : dark cycle (light period: 06:00 to 22:00 h) at 21.0 ºC (high temperature, HT) in semicontinous cultures. To simulate deep–sea temperature and light intensity, experimental treatments included low temperature (LT: 9.0 ºC), low light intensity (LL: 15 µmol photons m^{-2} s^{-1}) and combination of low temperature and low light intensity (LTLL: 9.0 ºC and 15 µmol photons m^{-2} s^{-1}) (Jordan and Winter, 2000; Beaufort et al., 2007). Therefore, there were four treatments in this study: (1) 9.0 ºC and 15 µmol photons m^{-2} s^{-1} (LTLL), (2) 9.0 ºC and 150 µmol photons m^{-2} s^{-1} (LTHL), (3) 21.0 ºC and 15 µmol photons m^{-2} s^{-1} (HTLL), (4) 21.0 ºC and 150 µmol photons m^{-2} s^{-1} (HTHL, control), and three replicates for each treatment.

Three strains were cultured in natural seawater obtained from the Pingtan Island, Southeast China. The seawater was first filtered using a membrane filter (0.45 µm pore size, CN-CA, Chuangwei), sterilized at 121ºC for 20 minutes, and enriched with 64 µmol L^{-1} NO^{3-}, 4 µmol L^{-1} PO_4^{3-}, f/8 concentrations for trace metal and vitamin solutions (Guillard and Ryther 1962). Then enriched seawater was aerated with sterile ambient air (PVDF 0.22 µm pore size, Simplepure, Haining) with about 400 µatm partial pressure of CO_2 for 24 hours, and sterilized by gentle pressure filtration (0.22 µm pore size, Polycap 75 AS, Whatman) and carefully pumped into autoclaved 500 mL

https://doi.org/10.5194/egusphere-2025-5131
Preprint. Discussion started: 18 November 2025

and 2000 mL polycarbonate (PC) bottles.

Three strains were cultured at 21.0 °C and 150 µmol photons m^{-2} s^{-1} with an initial cell concentration of about 3000 cells mL^{-1} and cultures were diluted every 3 days and maintained in exponential growth for 9 days with a minimum of 10 generations. After that, the cells of the same initial concentrations as above were transferred from 21.0 °C and 150 µmol photons m^{-2} s^{-1} (HTHL) to 21.0 °C and 15 µmol photons m^{-2} s^{-1} (HTLL) and to 9.0 °C and 150 µmol photons m^{-2} s^{-1} (LTHL), and then from 9.0 °C and 150 µmol photons m^{-2} s^{-1} to 9.0 °C and 15 µmol photons m^{-2} s^{-1} (LTLL). Cultures were diluted every 3 or 4 days, and maintained in exponential growth for 15 or 16 days under the HTLL and LTHL treatments, and for 32 days for *G. oceanica* strain and for 20 days for two *E. huxleyi* strains under the LTLL treatment, which were dependent on cell division rates per day of each strain (Figure S1). Culture bottles were mixed three times per day at 09:00 h, 14:00 h and 18:00 h. In the last day of the incubation under each treatment, subsamples were taken for measurements of cellular contents of total particulate carbon (TPC), particulate organic carbon (POC), nitrogen (PON) and phosphorus (POP), carbohydrate, lipid and chlorophyll (Chl) *a*.

2.2 Cell density measurement

After mixing, 2 mL samples for cell concentration measurement were taken daily at 14:00 h, and fixed with 10 µL Lugol's solution (a mixture of potassium iodide, iodine and sodium acetate). Then 1 mL samples were added into the counting chamber (Sedgwich–Rafter, S52, Graticules), and cell concentration was quantified by cell counting using a biological microscope (E100, Nikon Eclipse). Growth rate (μ) was calculated according to the equation: $\mu = (\ln N_1 - \ln N_0) / d$, where N_0 and N_1 were cell concentrations at the beginning and the end of a growth interval, and d was the duration

https://doi.org/10.5194/egusphere-2025-5131
Preprint. Discussion started: 18 November 2025

of the growth period in days (Wang et al., 2024).

2.3 Element content measurements

Samples for determinations of TPC (300 mL), POC and PON (300 mL), and POP (300 mL) contents were gently filtered onto GF/F filters (pre–combusted at 450 ºC for 5 hours) at 15:00 hour under each treatment. TPC, POC and POP samples were stored in the dark at –20 ºC. For POC measurements, samples were fumed with HCl for 12 hours to remove inorganic carbon. Then POC and TPC samples were dried at 60 ºC for 12 hours and analyzed using an Elemental CHNS analyser (Vario EL cube, GmbH, Germany). Cellular particulate inorganic carbon (PIC) content was calculated as the difference between TPC and POC (Fabry and Balch, 2010). To remove dissolved inorganic phosphorus from the GF/F filters, POP samples were rinsed three times with 5 mL 0.17 mol L^{-1} Na_2SO_4. After that, 2 mL 0.017 mol L^{-1} $MgSO_4$ solution was added onto filters. Then POP samples were dried at 90 ºC for 12 hours and combusted at 500 ºC for 6 hours to remove POC, then cooled and extracted by hydrolysis with 0.2 mol L^{-1} HCl (Solórzano and Sharp 1980). Phosphorus concentrations were determined using the ammonium molybdate method using adenosine–5–triphosphate disodium trihydrate (ATP007, Bioshop) as a standard.

2.4 Chlorophyll *a*, carbohydrate and lipid analyses

After mixing, samples for analyses of chlorophyll (Chl) *a* (100 mL), carbohydrate (500 mL) and lipid (300 mL) were obtained by filtering onto pre–combusted GF/F filters (at 450 ºC for 5 hours) at 15:00 hour under each treatment. Five milliliters of 90% acetone was used to extract the Chl *a* at 4 ºC for 24 hours. Then samples were centrifuged at 8000 rpm for 10 min at 4 ºC and the absorbances of the supernatant were determined

https://doi.org/10.5194/egusphere-2025-5131
Preprint. Discussion started: 18 November 2025

between 600–800 nm using a UV spectrophotometer (P5, Shanghai Mepada Instruments Ltd., China). Chl *a* concentration (μg L^{-1}) of sample was calculated as follows (Ritchie 2006).

$$\text{Chl } a = 11.93 \times (A_{664} - A_{750}) - 1.93 \times (A_{647} - A_{750})$$

where A_{647}, A_{664} and A_{750} were the absorbance values of supernatant at 647, 664 and 750 nm.

Carbohydrate samples were pretreated with 12.00 mol L^{-1} of sulfuric acid (H_2SO_4) in the dark for 1 hour, and then diluted by Milli–Q water to a final H_2SO_4 concentration of 1.20 mol L^{-1}. Then samples were sonicated for 5 min, vortexed for 30 s and boiled at 90.0 ºC for 3 hours (Pakulski and Benner, 1992). The concentration of monosaccharide was determined at 490 nm by phenol–sulfuric reaction with glucose as standard (Masuko et al., 2005).

Lipid samples were extracted with 2 mL dimethyl sulfoxide–methanol (v : v = 1 : 9), sonicated for 15 min, boiled at 60 ºC for 30 min. Then samples were centrifuged (5 min, 6000×g), and the oil–containing supernatants were transferred to a new tube (A, wight W_A) (Xu et al., 2020). The residue samples were treated with 4 mL ether–n–hexane (v : v = 1 : 1) for 1.5 h at 4 ºC. Then samples were centrifuged again and the supernatants were transferred to tube A again. The lipid–containing phase was dried using a nitrogen blower and then tube A was weighed (wight W_B) again. The lipid content was calculated as the difference between W_B and W_A.

2.5 Data Analysis

A two–way analysis of variance (ANOVA) was used to determine the main effect of temperature and light intensity and their interactions for all variables in this study. A Tukey post hoc test was performed to identify significant differences between two

https://doi.org/10.5194/egusphere-2025-5131
Preprint. Discussion started: 18 November 2025

levels of each treatment. A Shapiro–Wilk test was conducted to analyze the normality of residuals, and a Levene test was conducted to test for homogeneity of variances. The significant difference between treatments was set as $p \leq 0.05$. Data analysis and visualizations were made using R v.3.6.1 (R Core Team 2018) and packages ggplot2 v.3.2.0.

3 Results

3.1 Growth rate and cellular Chl *a* content

Low temperature and low light intensity acted synergistically to decrease growth rates of three strains, which can be seen by comparing growth rates in high temperature and high light intensity (HTHL) condition with those in high temperature and low light intensity (HTLL), low temperature and high light intensity (LTHL) and low temperature and low light intensity (LTLL) conditions (Figure 1a, b, c). Compared to HTHL, growth rates of *G. oceanica* NIES–1318 decreased by 34.28% ± 2.80% in HTLL, by 47.93% ± 0.70% in LTHL, and by 81.39% ± 2.64% in LTLL (Tukey, all $p < 0.01$) (Figure 1a). Similarly, compared to HTHL, growth rates of *E. huxleyi* PML B92/11 decreased by 37.54% ± 1.15% in HTLL, by 52.49% ± 0.94% in LTHL, and by 63.18% ± 2.65% in LTLL (Tukey, all $p < 0.01$) (Figure 1b). As to *E. huxleyi* RCC1266, compared to HTHL, growth rates decreased by 32.86% ± 3.47% in HTLL, by 47.96% ± 1.66% in LTHL, and by 64.01% ± 2.62% in LTLL (Tukey, all $p < 0.01$) (Figure 1c).

The effect of light intensity on cellular Chl *a* content depends on temperature. At high temperature (HT), compared to high light (HL) intensity, low light (LL) intensity increased the Chl *a* content of *E. huxleyi* PML B92/11 by 44.60% ± 10.97% (Tukey, $p < 0.01$) (Figure 1e), and did not significantly affect the Chl *a* contents of *G. oceanica*

https://doi.org/10.5194/egusphere-2025-5131
Preprint. Discussion started: 18 November 2025

NIES–1318 and *E. huxleyi* RCC1266 (Figure 1d, f). At low temperature (LT), compared to HL intensity, LL intensity did not significantly increase the Chl *a* contents of three strains (Tukey, all $p > 0.2$) (Figure 1d, e, f).

3.2 Cellular PIC, POC, PON and POP contents

The effect of light intensity on cellular PIC, POC and PON contents depends on temperature, which can be seen by comparing the PIC, POC and PON contents in the high temperature (HT) regimes with their paired low temperature (LT) regimes (Figure 2a, b, c). At HT, compared to HL intensity, low light (LL) intensity decreased the PIC contents by 38.17% ± 5.30% for *G. oceanica* NIES–1318 (Tukey, $p < 0.01$) (Figure 2a), by 28.96% ± 19.16% for *E. huxleyi* PML B92/11 (Tukey, $p = 0.11$) (Figure 2b), by 23.18% ± 7.15% for *E. huxleyi* RCC1266 (Tukey, $p = 0.04$) (Figure 2c). However, at LT, compared to HL intensity, LL intensity increased the PIC contents by 60.15% ± 11.16% for *G. oceanica* NIES–1318 (Tukey, $p < 0.01$) (Figure 2a), by 31.20% ± 14.85% for *E. huxleyi* PML B92/11 (Tukey, $p = 0.79$) (Figure 2b), by 109.18% ± 32.21% for *E. huxleyi* RCC1266 (Tukey, $p = 0.04$) (Figure 2c).

At HT, compared to HL intensity, low light (LL) intensity decreased the POC contents by 28.78% ± 4.26% for *G. oceanica* NIES–1318 ($p < 0.01$) (Figure 2d), by 38.53% ± 7.13% for *E. huxleyi* PML B92/11 ($p < 0.01$) (Figure 2e), and by 31.72% ± 6.29% for *E. huxleyi* RCC1266 ($p < 0.01$) (Figure 2f). At LT, compared to HL intensity, LL intensity did not significantly affect the POC contents of three strains (all $p > 0.5$) (Figure 2d, e, f). The response of PON contents to low temperature and low light conditions was similar to that of PIC contents. At HT, compared to HL intensity,

https://doi.org/10.5194/egusphere-2025-5131
Preprint. Discussion started: 18 November 2025

LL intensity decreased the PON contents by 9.23% ± 10.02% for *G. oceanica* NIES–1318 ($p > 0.50$) (Figure 2g), by 18.65% ± 4.16% for *E. huxleyi* PML B92/11 ($p < 0.01$) (Figure 2h), and by 18.87% ± 1.51% for *E. huxleyi* RCC1266 ($p = 0.21$) (Figure 2i). However, at LT, compared to HL intensity, LL intensity increased the PON contents by 30.72% ± 15.64% for *G. oceanica* NIES–1318 ($p = 0.12$) (Figure 2g), by 29.16% ± 10.93% for *E. huxleyi* PML B92/11 ($p = 0.03$) (Figure 2h), and by 49.74% ± 31.57% for *E. huxleyi* RCC1266 ($p = 0.12$) (Figure 2i). Interestingly, compared to HTLL, low temperature and low light intensity did not significantly affect the POP contents of three strains (all $p > 0.05$) (Figure 2j,k,l).

3.3 PIC : POC, POC : PON, POC: POP and PON : POP ratios

The effects of temperature and light intensity on the PIC : POC ratio are strain–specific (Figure 3a,b,c). As to *G. oceanica* NIES–1318, compared to HTHL, PIC : POC ratio didn't be affected significantly in HTLL and LTHL, whereas increased by 63.15% ± 13.29% in LTLL ($p < 0.01$) (Figure 3a). As to *E. huxleyi* PML B92/11, compared to HTHL, PIC : POC ratio didn't be affected significantly in HTLL, LTHL and LTLL (Figure 3b) (all $p > 0.20$). As to *E. huxleyi* RCC1266, compared to HTHL, PIC : POC ratio didn't be affected significantly in HTLL and LTLL, and decreased by 63.38% ± 6.62% in LTHL ($p < 0.01$) (Figure 3c).

Low temperature and low light intensity acted synergistically to decrease the POC : PON ratios and POC : POP ratios of three strains, which can be seen by comparing the POC : PON and POC : POP ratios under the HTHL treatment with HTLL, LTHL and LTLL treatments (Figure 3d–i). Compared to HTHL, POC : PON ratio of *G. oceanica* NIES–1318 decreased by 20.97% ± 9.33% in HTLL ($p = 0.07$), by 34.72% ± 4.93%

https://doi.org/10.5194/egusphere-2025-5131
Preprint. Discussion started: 18 November 2025

in LTHL ($p < 0.01$), and by 56.21% ± 6.32% in LTLL ($p < 0.01$) (Figure 3d). As to *E. huxleyi* PML B92/11, compared to HTHL, POC : PON ratio decreased by 24.69% ± 1.76% in HTLL, by 20.42% ± 2.49% in LTHL, and by 45.61% ± 7.37% in LTLL (all $p < 0.05$) (Figure 3e). As to *E. huxleyi* RCC1266, compared to HTHL, POC : PON ratio decreased by 16.00% ± 3.81% in HTLL ($p = 0.13$), by 14.66% ± 3.16% in LTHL ($p = 0.18$), and by 51.87% ± 9.43% in LTLL ($p < 0.01$) (Figure 3f). At HT, compared to HL intensity, low light intensity decreased the POC : POP ratios by 24.46% ± 14.33% for *G. oceanica* NIES–1318 ($p = 0.06$) (Figure 3g), by 33.05% ± 5.27% for *E. huxleyi* PML B92/11 ($p < 0.01$) (Figure 3h), and by 24.50% ± 8.83% for *E. huxleyi* RCC1266 ($p < 0.01$) (Figure 3i). At LT, compared to HL intensity, low light intensity did not significantly affect the POC : POP ratios of three strains (Figure 3g, h, i). Please note that compared to HTHL, POC : POP ratios of three strains decreased by 52.11%–59.61% in LTHL and LTLL (all $p < 0.01$).

The effect of light intensity on the PON : POP ratio depends on temperature, which can be seen by comparing the PON : POP ratio in the HT regimes with their paired LT regimes (Figure 3j, k, l). Compared to HL intensity, at HT, low light (LL) intensity did not significantly decrease the PON : POP ratios of three strains, whereas at LT, it increased the PON : POP ratios by 52.88%–57.29% (Figure 3j,k,l) (both $p < 0.05$ for *G. oceanica* NIES–1318 and *E. huxleyi* PML B92/11; $p = 0.08$ for *E. huxleyi* RCC1266).

3.4 Cellular carbohydrate and lipid contents

Cellular carbohydrate and lipid contents were mainly affected by light intensity, which can be seen by comparing the carbohydrate and lipid contents in the HL intensity with their paired LL intensity (Figure 4). Compared to HL intensity, in LL intensity, the

https://doi.org/10.5194/egusphere-2025-5131
Preprint. Discussion started: 18 November 2025

carbohydrate contents were significantly lower for three strains regardless of levels of temperature for the range used here (Figure 4a,b,c). Compared to HL intensity, at HT, low light intensity decreased the carbohydrate contents by 79.76%–82.75% of three strains (all $p < 0.01$), and at LT, it decreased the carbohydrate contents by 84.77%–87.72% (all $p < 0.01$) (Figure 4a,b,c). Similarly, compared to HL intensity, at HT, low light intensity decreased the lipid contents by 63.34%–68.70% of three strains (all $p < 0.01$), and at LT, it decreased the lipid contents by 75.77%–85.10% (all $p < 0.01$) (Figure 4d,e,f).

4 Discussion

We propose that under extreme low temperature and low light intensity (LTLL), coccolithophores slow their metabolism, leading to reductions in growth rate, POC, POP, carbohydrate and lipid contents. Our results reveal a specific acclimation strategy: energy conservation is prioritized through the initial reduction of carbohydrate and lipid content, followed by a decrease in growth rate (Figure 4). Furthermore, carbohydrates and lipids were primarily light–dependent, while PON (proxy for protein) was temperature–dependent. Analysis of POC : PON : POP ratios showed that POC decreased more steeply than PON, and more steeply than POP only at high temperature (Figure 3). Notably, at low temperature, POC and POP were light–insensitive, whereas PON was inhibited by high light intensity. Collectively, these results indicate that coccolithophores acclimate to LTLL conditions by precisely regulating their biomolecular composition, elemental stoichiometry and growth (Zhang et al., 2021).

Compared to LTLL condition, in low temperature and high light intensity (LTHL), both carbohydrates and lipids increased threefold, whereas the POC content did not increase significantly. This indicates that proteins have decreased, which is also

https://doi.org/10.5194/egusphere-2025-5131
Preprint. Discussion started: 18 November 2025

corroborated by the reduction in PON content (Figures 2, 4). The reasons could be that at 9 ºC, the overall cellular metabolism is certainly slow. At this point, 150 µmol photons m^{-2} s^{-1} of PAR is excessive (Jin et al., 2019). The cell stores the excess energy in the form of carbohydrates and lipids, which also serves as a protective mechanism (Zhang et al., 2021). Typically, the contents of POC, PIC and PON exhibit an optimal light intensity response curve (Zhang et al., 2015). Under high temperature conditions, high light increases POC and PON; however, under low temperature conditions, it reduces the PON content (Figure 2). This also implies that low temperature lowers the optimal light intensity for PON synthesis, and reduces the coccolithophore's tolerance to high light (Gafar et al., 2018). In addition, under low temperature, the Calvin cycle is slow, leading to slow carbon fixation, which requires less energy and then lower Chl *a* content (Figure 1). Especially, under high light conditions, cells are more prone to downregulate the content of light–harvesting antenna proteins, thereby reducing the absorption of excess light by these antenna proteins, making an important contribution to decreased PON (McKew et al., 2013). The significant lower Chl *a* content in high temperature and high light intensity (HTHL) than that in high temperature and low light intensity (HTLL) was only found for *E. huxleyi* PML B92/11, which suggests that the response of Chl *a* content to increasing light intensity varies between species or strains (Figure 1e).

Previous studies reported unchanged or increased POC contents at 14 ºC than 18 ºC (Borchard et al., 2011), at 15 ºC than 18 ºC or 20 ºC (Tong et al., 2019; Torres–Romero et al., 2024), and at 20 ºC than 24 ºC (Feng et al., 2008). These findings are inconsistent with our results which shows decreased POC contents at 9 ºC than 21 ºC (Figure 2). One key reason is that the inhibitory effect of 9 ºC on the photosynthetic carbon fixation efficiency and growth rate of algae is significantly larger than that of 14 ºC or 15 ºC

https://doi.org/10.5194/egusphere-2025-5131
Preprint. Discussion started: 18 November 2025

(Shen et al., 2025). In addition, the variation in POC and POP contents between strains may have been masked by the large gradients of temperature or light intensity used in this study.

Interestingly, the combination of low temperature and low light did not significantly affect the POP content in coccolithophores (Figure 2j–l). The possible reasons are as follows: while low light intensity directly limits photosynthetic efficiency, low temperature simultaneously suppresses the respiratory rate, leading to a synchronous reduction in adenosine triphosphate (ATP) synthesis and overall energy consumption (Jin et al., 2019; Strzepek et al., 2019). This effect helps maintain a dynamic balance between phosphorus consumption (e.g. for ATP synthesis) and supply (e.g. phosphorus uptake) (Dyhrman, 2016). Meanwhile, low temperature and low light intensity inhibit energy–intensive processes such as carbohydrate or lipid synthesis and cell division (Figures 4, 1). Under these conditions, coccolithophores prioritize phosphorus allocation to critical biomolecules. For instance, phosphorus is preferentially allocated to nucleic acids (DNA or RNA) and membrane phospholipids, while investment in non–essential metabolic pathways (e.g., secondary metabolite synthesis) is reduced (Shemi et al., 2016). This strategy allows the cells to maintain the core components of POP unchanged even when overall metabolism slows down (Shemi et al., 2016). From an ecological perspective, the stability of POP under low temperature and low light conditions enables coccolithophores to maintain ecological competitiveness in high–latitude regions or deep–water layers (Perrin et al., 2016). This adaptability may be one of the kay factors that allowed them to survive multiple glacial–interglacial cycles throughout geological history (Tangunan et al., 2021).

While calcification is known to be energy–dependent and enhanced by high light intensity at warm temperatures (Triccas et al., 2025), we observed a counterintuitive

https://doi.org/10.5194/egusphere-2025-5131
Preprint. Discussion started: 18 November 2025

result under cold stress: high light intensity reduced the PIC content (Figure 2a–c). This challenges the conversional view that cells under energy limitation (low light) should reduce calcification (Zhang et al., 2015). We propose several mechanisms: low temperature (LT) reduces the repair capacity of photosynthetic structures, and then photoinhibition at LT is more likely to damage cellular membranes, disrupting ion transport (Ca^{2+} or HCO_3^-) and homeostasis critical for calcification (Strzepek et al., 2019; Triccas et al., 2025). Alternatively, under low temperature and low light intensity, more coccoliths might act as micro–lenses to concentrate light on chloroplasts, making them beneficial (Young et al., 1999). Ecologically, high PIC contents may defend against grazers and a high PIC : POC ratio could promote sinking, and enhance carbon sequestration in the deep sea (Poulton et al., 2014; Rigual–Hernández et al., 2020). Notably, PIC content showed significant strain–specific variation under the same treatment, e.g. high temperature and high light intensity, highlighting how such diversity allows coccolithophores to colonize diverse marine habitats from sunlit surfaces to the deep sea (Rigual–Hernández et al., 2018).

Three coccolithophore strains were found to be capable of calcification in the deep–sea environment characterized by low temperature and limited light (Figure 2). This implies that significant carbon export may occur in deeper waters (Malinverno et al., 2003; Rigual–Hernández et al., 2018). Calcification activities in the deep sea exert distinct influences on the marine carbon chemical system compared to those in surface waters, necessitating a re–evaluation of their impacts (Rigual–Hernández et al., 2020). Neglecting the contribution of deep–sea coccolithophores may lead to a severe underestimation of global marine carbonate production (Rigual–Hernández et al., 2018). On the other hand, studying the survival and adaptation capabilities of phytoplankton, represented by coccolithophores, under low temperature and low light conditions can

https://doi.org/10.5194/egusphere-2025-5131
Preprint. Discussion started: 18 November 2025

enhance our understanding of the environmental tolerance limits of photosynthetic organisms (Rigual–Hernández et al., 2018; Chauhan et al., 2024). This provides important insights into the adaptive strategies of life under extreme conditions (Rigual–Hernández et al., 2018). In summary, research on the adaptive features of coccolithophores to the deep sea's cold and dark environment reveals that critical forces driving global ecosystems persist even in the seemingly barren deep ocean (Perrin et al., 2016).

https://doi.org/10.5194/egusphere-2025-5131
Preprint. Discussion started: 18 November 2025

References

Beaufort, L., Couapel, M., Buchet, N., and Claustre, H.: Calcite production by coccolithophores in the South East Pacific Ocean: from desert to jungle, Biogeosciences Discuss., 4, 3267–3299, doi: 10.5194/bgd-4-3267-2007, 2007.

Borchard, C., Borges, A. V., Händel, N., and Engel, A.: Biogeochemical response of *Emiliania huxleyi* (PML B92/11) to elevated CO_2 and temperature under phosphorus limitation: A chemostat study, J. Exp. Mar. Biol. Ecol., 410, 61–71, https://doi.org/10.1016/j.jembe.2011.10.004, 2011.

Chauhan, N., Barton, S., Zarkogiannis, S., and Rickaby, R. E. M.: Light quality induces a shift in coccosphere morphology in *Scyphosphaera apsteinii*, J. Plankton. Res., 46, 383–386, doi: 10.1093/plankt/fbae032, 2024.

Conte, M. H., Sicre, M. A., Rühlemann, C., Weber, J. C., Schulte, S., Schulz–Bull, D., and Blanz, T.: Global temperature calibration of the alkenone unsaturation index (U_{37}^{K}) in surface waters and comparison with surface sediments, Geochem., Geophy., Geosys., 7, Q02005, doi: 10.1029/2005GC001054, 2006.

Conte, M. H., Thompson, A., Lesley, D., and Harris, R. P: Genetic and physiological influences on the alkenone/alkenoate versus growth temperature relationship in *Emiliania huxleyi* and *Gephyrocapsa oceanica*, Geochim. Cosmochim. Ac., 62, 51–68, doi: 10.1016/S0016-7037(97)00327-X, 1998.

Dedman, C. J., Barton, S., Fournier, M., and Richaby, R. E. M.: The cellular response to ocean warming in *Emiliania huxleyi*, Front. Microbiol., 14, 1177349, doi: 10.3389/fmicb.2023.1177349, 2023.

Dyhrman, S. T.: Nutrients and their acquisition: phosphorus physiology in microalgae, in: The physiology of microalgae, edited by: Borowitzka, M. A., Beardall, J., and

https://doi.org/10.5194/egusphere-2025-5131
Preprint. Discussion started: 18 November 2025

Raven, J. A., Springer, Heidelberg, Germany, 155–183, https://doi.org/10.1007/978-3-319-24945-2, 2016.

Fabry, V. J., and Balch, W. M.: Direct measurements of calcification rates in planktonic organisms, in: Guide to best practices for ocean acidification research and data reporting, edited by Riebesell, U., Fabry, V. J., Hansson, L., and Gattuso, J. P., Luxembourg, Publications Office of the European Union, 201–212, https://doi.org/10.2777/66906, 2010.

Feng, Y., Warner, M. E., Zhang, Y., Sun, J., Fu, F., Rose, J. M., and Hutchins, D. A.: Interactive effects of increased pCO_2, temperature and irradiance on the marine coccolithophore *Emiliania huxleyi* (Prymnesiophyceae), Eur. J. Phycol., 43, 87–98, https://doi.org/10.1080/09670260701664674, 2008.

Gafar, N. A., Eyre, B. D., and Schulz, K. G.: A conceptual model for projecting coccolithophorid growth, calcification and photosynthetic carbon fixation rates in response to global ocean change, Front. Mar. Sci., 4, 433, doi: 10.3389/fmars.2017.00433, 2018.

Guillard, R. R. L., and Ryther, J. H.: Studies of marine planktonic diatoms. I. Cyclotella nana Hustedt and Detonula confervacea Cleve. Can. J. Microbiol., 8, 229–239, doi:10. 1139/m62-029, 1962.

Hernández–Almeida, I., Krumhardt K. M., Zhang H., and Stoll H. M.: Estimation of physiological factors controlling carbon isotope fractionation in coccolithophores in photic zone and core–top samples, Geochem. Geophy. Geosy., 21, e2020GC009272, doi: 10.1029/2020GC009272, 2020.

Horváth, G., and Varjú, D.: Polarized light in animal vision: polarization patterns in nature, Springer, Berlin, 319–324, https:doi//10.1007/978-3-662-09387-0, 2004.

Jin, P., Liu, N., and Gao, K.: Physiological responses of a coccolithophore to multiple

https://doi.org/10.5194/egusphere-2025-5131
Preprint. Discussion started: 18 November 2025

environmental drivers, Mar. Pollut. Bull., 146, 225–235, doi:10.1016/j.marpolbul.2019.06.032, 2019.

Jordan, R. W., and Winter, A.: Assemblages of coccolithophorids and other living microplankton off the coast of Puerto Rico during January–May 1995, Mar. Micropaleontol., 39, 113–130, dio: 10.1016/S0377-8398(00)00017-7, 2000.

Li, S., Zhu, J., Jin, X., Feng, Y., Jiao, N., and Zhang, W.: Multifaceted contributions of coccolithophores to ocean carbon export, Ocean-Land-Atmos. Res., 3, Article0049, doi: 10.34133/olar.0049, 2024.

Malinverno, E., Ziveri, P., and Corselli, C.: Coccolithophorid distribution in the Ionian Sea and its relationship to eastern Mediterranean circulation during late fall to early winter 1997, J. Geophys. Res., 108(C9), 8115, doi: 10.1029/2002JC001346, 2003.

Masuko, T., Minami, A., Iwasaki, N., Majima, T., Nishimura, S. I., and Lee, Y. C.: Carbohydrate analysis by a phenolsulfuric acid method in microplate format, Anal. Biochem., 339, 69–72. doi:10.1016/j.ab.2004.12.001, 2005.

McKew, B. A., Lefebvre, S. C., Achterberg, E. P., Metodieva, G., Raines, C. A., Metodiev, M. V., and Geider, R. J.: Plasticity in the proteome of *Emiliania huxleyi* CCMP 1516 to extremes of light is highly targeted, New Phytol., 200, 61–73, doi: 10.1111/nph.12352, 2013.

Pakulski, J. D., and Benner, R: An improved method for the hydrolysis and MBTH analysis of dissolved and particulate carbohydrates in seawater, Mar. Chem., 40, 143–160, doi:10.1016/0304-4203(92)90020-B, 1992.

Perrin, L., Probert, I., Langer, G., and Aloisi, G.: Growth of the coccolithophore *Emiliania huxleyi* in light– and nutrient–limited batch reactors: relevance for the BIOSOPE deep ecological niche of coccolithophores, Biogeosciences, 13, 5983–

https://doi.org/10.5194/egusphere-2025-5131
Preprint. Discussion started: 18 November 2025

6001, doi: 10.5194/bg-13-5983-2016, 2016.

Petrou, K., Kranz, S. A., Trimborn, S., Hassler, C. S., Ameijeiras, S. B., Sackett, O., Ralph, P. J., and Davidson, A. T.: Southern Ocean phytoplankton physiology in a changing climate, J. Plant Physiol., 203, 135–150, doi: 10.1016/j.jplph.2016.05.004, 2016.

Poulton, A. J., Stinchcombe, M. C., Achterberg, E. P., Bakker, D. C. E., Dumousseaud, C., Lawson, H. E., Lee, G. A., Richier, S., Suggett, D. J., and Young, J. R.: Coccolithophores on the north–west European shelf: calcification rates and environmental controls, Biogeosciences, 11, 3919–3940, doi: 10.5194/bg-11-3919-2014, 2014.

R Core Team: The R foundation for statistical computing platform, x86_64-w64-mingw32/x64, available at: https://cran.r-project.org/bin/windows/base/old/3.5.0/ (28 February 2020), 2018.

Rigual–Hernández, A. S., Trull, T. W., Nodder, S. D., Flores, J. A., Bostock, H., Abrantes, F., Eriksen, R. S., Sierro, F. J., Davies, D. M., Ballegeer, A. M., Fuertes, M. A., and Northcote, L. C.: Coccolithophore biodiversity controls carbonate export in the Southern Ocean, Biogeosciences, 17, 245–263, 2020.

Rigual–Hernández, A., Flores, J. A., Sierro, F. J., Fuertes, M. A., Cros, L., and Trull, T. W.: Coccolithophore populations and their contribution to carbonate export during an annual cycle in the Australian section of the Antarctic zone, Biogeosciences, 15, 1843–1862, doi: 10.5194/bg-15-1843-2018, 2018.

Ritchie, R. J.: Consistent sets of spectrophotometric chlorophyll equations for acetone, methanol and ethanol solvents, Photosynth Res., 89, 27–41, doi: 10.1007/s11120-006-9065-9, 2006.

Sage, R. F.: Variation in the kcat of Rubisco in C3 and C4 plants and some implications

https://doi.org/10.5194/egusphere-2025-5131
Preprint. Discussion started: 18 November 2025

for photosynthetic performance at high and low temperature, J. Experimental Botany, 53: 609–620, doi: 10.1016/j.jplph.2016.05.004, 2016.

Shemi, A., Schatz, D., Fredricks, H. F., Van Mooy, B. A. S., Porat, Z., and Vardi, A.: Phosphorus starvation induces membrane remodeling and recycling in *Emiliania huxleyi*, New Phytol., 211, 886–898, doi: 10.1111/nph.13940, 2016.

Shen, L., Ren, F., Wang, Y. C., Li, Z., Zheng, M., Li, X., Fan, W., Yang, Y., Sang, M., Liu, C. Han, G., Qin, S., Fan, J., Tian, L., Kuang, T., Shen, J. R., and Wang, W.: Structure and function of a huge photosystem I-fucoxanthin chlorophyll supercomplex from a coccolithophore, Science, 389, eadv2132, doi: 10.1126/science.adv2132, 2025.

Shen, Y., Jiang, R., Chang, J., Cai, L., Zhu, Y., Yin, Y., Shao, L., Wu, M., Zhang, J., and He, P.: The effect of temperature on the photosynthetic carbon fixation efficiency of sessile macroalgae in the mussel farming area of Guoqi Island through stable isotope, Mar. Environ. Res., 209, 107190, doi: 10.1016/j.marenvres.2025.107190, 2025.

Skeffington, A., Fischer, A., Sviben, S., Brzezinka, M., Górka, M., Bertinetti, L., Woehle, C., Huettel, B., Graf, A., and Scheffel, A.: A joint proteomic and genomic investigation provides insights into the mechanism of calcification in coccolithophores, Nature Commun., 24, 3749, doi: 10.1038/s41467-023-39336-1

Solorzano, L., and Sharp, J. H.: Determination of total dissolved phosphorus and particulate phosphorus in nature waters, Limnol. Oceanogr., 25, 754–758, doi:10.4319/lo.1980.25.4.0754, 1980.

Strzepek, R. F., Boyd, P. W., and Sunda, W. G.: Photosynthetic adaptation to low iron, light, and temperature in Southern Ocean phytoplankton, Proc. Nat. Acad. Sci. U. S., 116, 4388–4393, doi: 10.1073/pnas.1810886116, 2019.

https://doi.org/10.5194/egusphere-2025-5131
Preprint. Discussion started: 18 November 2025

570 Tangunan, D., Berke, M. A., Cartagena-Sierra, C., Flores, J. A., Gruetzner, J., Jiménez-
571 Espejo, F., LeVay, L. J., Baumann, K. H., Romero, O., Saavedra–Pellitero, M.,
572 Coenen, J. J., Starr, A., Hemming, S. R., Hall, I. R., E and Expedition 361 Science
573 Party: Strong glacial–interglacial variability in upper ocean hydrodynamics,
574 biogeochemistry, and productivity in the southern Indian Ocean, Commun. Earth
575 Environ., 2, 80, doi: 10.1038/s43247-021-00148-0, 2021.
576 Tong, S., Hutchins, D. A., and Gao, K.: Physiological and biochemical responses of
577 *Emiliania huxleyi* to ocean acidification and warming are modulated by UV
578 radiation, Biogeosciences, 16, 561–572, https://doi.org/10.5194/bg-16-561-2019,
579 2019.
580 Torres–Romero, I., Clark, A. J., Wijker, R. S., Jaggi, M., Zhang, H., and Stoll, H. M.:
581 Temperature–dependent carbon isotope fractionation in coccolithophores, Front.
582 Earth Sci., 12, 1331179, doi: 10.3389/feart.2024.1331179, 2024.
583 Triccas, A., Chevrier, D. M., Verezhak, M., Ihli, J., Guizar-Sicairos, M., Holler, M.,
584 Scheffel, A., Ozaki, N., Chamard, V., Wood, R., Grünewald, T. A., and Nudelman,
585 F.: Dynamic change of calcium-rich compartments during coccolithophore
586 biomineralization, Sci. Adv., 11, eadv0618, doi: 10.1126/sciadv.adv0618, 2025.
587 Triccas, A., Chevrier, D. M., Verezhak, M., Ihli, J., Guizar–Sicairos, M., Holler, M.,
588 Scheffel, A., Ozaki, N., Chamard, V., Wood, R., Grünewald, T. A., and Nudelman,
589 F.: Dynamic change of calcium–rich compartments during coccolithophore
590 biomineralization, Sci. Adv., 11, eadv0618, doi: 10.1126/sciadv.adv0618, 2025.
591 Wang, D., Gao, X., Wang, X., Yuan, X., Guo, X., Zhang, Y., Xu, K., and Li, Z.: Diverse
592 thermal responses of the growth, photosynthesis, lipid and fatty acids in the
593 terrestrial oil–producing microalga *Vischeria* sp. WL1, J. Appl. Phycol., 36, 29–
594 39, doi:10.1007/s10811-023-03152-3, 2024.

https://doi.org/10.5194/egusphere-2025-5131
Preprint. Discussion started: 18 November 2025

595 Xu, J., Li, T., Li, C. L., Zhu, S. N., Wang, Z. M., and Zeng, E. Y.: Lipid accumulation
596 and eicosapentaenoic acid distribution in response to nitrogen limitation in
597 microalga *Eustigmatos vischeri* JHsu-01 (Eustigmatophyceae), Algal Res., 48,
598 101910, doi: 10.1016/j.algal.2020,101910, 2020.
599 Young, J. N., Goldman, J. A. L., Kranz, S. A., Tortell, P. D., and Morel, F. M. M.: Slow
600 carboxylation of Rubisco constrains the rate of carbon fixation during Antarctic
601 phytoplankton blooms, New Phytol., 205, 172–181, doi: 10.1111/nph.13021, 2015.
602 Young, J. R., Davis, S. A., Bown, P. R., and Mann, S.: Coccolith ultrastructure and
603 biomineralisation, J. Struct. Biol., 126, 195–215, doi: 10.1006/jsbi.1999.4132,
604 1999.
605 Zhang, Y., and Gao, K.: Photosynthesis and calcification of the coccolithophore
606 *Emiliania huxleyi* are more sensitive to changed levels of light and CO_2 under
607 nutrient limitation, J. Photochem. Photobiol. B: Biol., 217, 112145, doi:
608 10.1016/j.jphotobiol.2021.112145, 2021.
609 Zhang, Y., Bach, L. T., Schulz, K. G., and Riebesell, U.: The modulating effect of light
610 intensity on the response of the coccolithophore *Gephyrocapsa oceanica* to ocean
611 acidification, Limnol. Oceanogr., 60, 2145–2157, doi: 10.1002/lno.10161, 2015.
612 Zhang, Y., Collins, S., and Gao, K.: Reduced growth with increased quotas of
613 particulate organic and inorganic carbon in the coccolithophore *Emiliania huxleyi*
614 under future ocean climate change conditions, Biogeosciences, 17, 6357–6375,
615 doi:10.5194/bg-17-6357-2020, 2020.
616 Zhang, Y., Li, Z., Schulz, K. G., Hu, Y., Irwin, A. J., and Finkel, Z. V.: Growth-
617 dependent changes in elemental stoichiometry and macromolecular allocation in
618 the coccolithophore *Emiliania huxleyi* under different environmental conditions,
619 Limnol. Oceanogr., 66, 2999–3009, doi: 10.1002/lno.11854, 2021.

https://doi.org/10.5194/egusphere-2025-5131
Preprint. Discussion started: 18 November 2025

Data availability. The data are available upon request to the corresponding author (Yong Zhang)

Author contributions. YZ and JS designed the experiment. YW performed the experiment. WK and JS analyzed the data and wrote the first manuscript. All authors improved and reviewed the manuscript. JS, WK and YW contributed equally to this work.

Competing interests. The authors declare that they have no conflict of interest.

Financial support. This study was supported by the National Natural Science Foundation of China (No. 32270397), Natural Science Foundation of Xinjiang Uygur Autonomous Region (No. 202501A54), the Xinjiang Normal University Landmark Achievements Cultivation Project (XJNUZBS2401), the Tianchi Talent Program in Xinjiang Uyghur Autonomous Region, and by Hubei Provincial Department of Education Scientific Research Plan Guidance Project (B2019435), China; Natural Science Foundation of Fujian Province (2023J01290), China; and the "GeoX" Interdisciplinary, Research Funds for the Frontiers Science Center for Critical Earth Material Cycling, Nanjing University (020614380194), China.

https://doi.org/10.5194/egusphere-2025-5131
Preprint. Discussion started: 18 November 2025

Figure Legends

Figure 1. Under the treatments of low temperature (LT, 9 ºC) and low light (LL, 15 μmol photons m^{-2} s^{-1}), LTHL (9 ºC, 150 μmol photons m^{-2} s^{-1}), HTLL (21 ºC, 15 μmol photons m^{-2} s^{-1}) and HTHL (21 ºC, 150 μmol photons m^{-2} s^{-1}), growth rates and cellular contents of chlorophyll *a* of *Gephyrocapsa oceanica* NIES–1318, *Emiliania huxleyi* PML B92/11 and *E. huxleyi* RCC1266. Data are presented as mean ± standard deviation for three replicates (n = 3). Different letters (a, b, c, d) represent significant differences between treatments (Tukey, $p < 0.05$).

Figure 2. Under the treatments of low temperature (LT, 9 ºC) and low light (LL, 15 μmol photons m^{-2} s^{-1}), LTHL (9 ºC, 150 μmol photons m^{-2} s^{-1}), HTLL (21 ºC, 15 μmol photons m^{-2} s^{-1}) and HTHL (21 ºC, 150 μmol photons m^{-2} s^{-1}), cellular contents of particulate inorganic carbon (PIC), particulate organic carbon (POC), particulate organic nitrogen (PON), particulate organic phosphorus (POP) of *Gephyrocapsa oceanica* NIES–1318, *Emiliania huxleyi* PML B92/11 and *E. huxleyi* RCC1266. Data are presented as mean ± standard deviation for three replicates (n = 3). Different letters (a, b, c, d) represent significant differences between treatments (Tukey, $p < 0.05$).

Figure 3. Under the treatments of low temperature (LT, 9 ºC) and low light (LL, 15 μmol photons m^{-2} s^{-1}), LTHL (9 ºC, 150 μmol photons m^{-2} s^{-1}), HTLL (21 ºC, 15 μmol photons m^{-2} s^{-1}) and HTHL (21 ºC, 150 μmol photons m^{-2} s^{-1}), the ratios of PIC : POC, POC : PON, POC : POP, PON : POP of *Gephyrocapsa oceanica* NIES–1318, *Emiliania huxleyi* PML B92/11 and *E. huxleyi* RCC1266. Data are presented as mean ± standard deviation for three replicates (n = 3). Different letters (a, b, c, d) represent significant differences between treatments (Tukey, $p < 0.05$).

https://doi.org/10.5194/egusphere-2025-5131
Preprint. Discussion started: 18 November 2025

Figure 4. Under the treatments of low temperature (LT, 9 ºC) and low light (LL, 15 µmol photons m^{-2} s^{-1}), LTHL (9 ºC, 150 µmol photons m^{-2} s^{-1}), HTLL (21 ºC, 15 µmol photons m^{-2} s^{-1}) and HTHL (21 ºC, 150 µmol photons m^{-2} s^{-1}), cellular contents of carbohydrate and lipid of *Gephyrocapsa oceanica* NIES–1318, *Emiliania huxleyi* PML B92/11 and *E. huxleyi* RCC1266. Data are presented as mean ± standard deviation for three replicates (n = 3). Different letters (a, b, c, d) represent significant differences between treatments (Tukey, $p < 0.05$).

Figure S1. Under the treatments of low temperature (LT, 9 ºC) and low light (LL, 15 µmol photons m^{-2} s^{-1}), LTHL (9 ºC, 150 µmol photons m^{-2} s^{-1}), HTLL (21 ºC, 15 µmol photons m^{-2} s^{-1}) and HTHL (21 ºC, 150 µmol photons m^{-2} s^{-1}), growth curves of *Gephyrocapsa oceanica* NIES–1318, *Emiliania huxleyi* PML B92/11 and *E. huxleyi* RCC1266. Data are presented as mean ± standard deviation for three replicates (n = 3).

https://doi.org/10.5194/egusphere-2025-5131
Preprint. Discussion started: 18 November 2025

Table 1. Results of two–way ANOVAs of the impacts of temperature (T), light intensity (L) and their interaction (T×L) on growth rate (μ), chlorophyll (Chl) *a*, PIC, POC, PON and POP contents, PIC : POC ratio, POC : PON ratio, POC : POP ratio, PON : POP ratio, as well as carbohydrate (Carbo) and lipid contents.

		G. oceanica NIES–1318		*E. huxleyi* PML B92/11		*E. huxleyi* RCC1266	
	Factor	*F* value	*p* value	*F* value	*p* value	*F* value	*p* value
μ	T	1950.0	<0.001	1362.4	<0.001	1006.3	<0.001
	L	991.0	<0.001	518.8	<0.001	384.8	<0.001
	T×L	0.16	=0.702	161.5	<0.001	45.60	<0.001
Chl *a*	T	11.9	=0.009	66.6	<0.001	3.6	=0.094
	L	2.9	=0.128	39.4	<0.001	1.5	=0.261
	T×L	1.5	=0.254	18.3	=0.003	0.2	=0.669
PIC	T	168.6	<0.001	35.6	<0.001	185.2	<0.001
	L	10.2	=0.013	1.4	=0.267	0.7	=0.427
	T×L	103.2	<0.001	6.3	=0.037	14.9	=0.005
POC	T	358.7	<0.001	552.6	<0.001	215.3	<0.001
	L	40.2	<0.001	107.4	<0.001	31.4	<0.001
	T×L	19.8	=0.002	69.4	<0.001	13.2	=0.007
PON	T	34.1	<0.001	289.8	<0.001	33.9	<0.001
	L	0.8	=0.397	1.8	=0.221	0.1	0.793
	T×L	7.5	=0.025	40.2	<0.001	11.3	=0.010
POP	T	5.4	=0.049	15.1	=0.005	9.6	=0.015
	L	1.1	=0.324	4.4	=0.068	0.8	=0.394
	T×L	0.3	=0.618	0.2	=0.673	0.5	=0.516
PIC : POC	T	19.5	=0.002	0.9	=0.360	26.9	=0.001
	L	17.2	=0.003	3.8	=0.086	17.8	=0.003
	T×L	35.4	<0.001	0.9	=0.379	7.3	=0.027
POC : PON	T	50.5	<0.001	25.2	=0.001	30.6	=0.001
	L	18.2	=0.003	36.1	<0.001	34.4	<0.001
	T×L	0.1	=0.917	0.1	=0.961	5.3	=0.050
POC : POP	T	57.0	<0.001	101.8	<0.001	203.7	<0.001
	L	3.7	=0.090	14.1	=0.006	28.2	=0.001
	T×L	5.8	=0.043	17.6	=0.003	8.3	=0.020
PON : POP	T	1.6	=0.245	41.5	<0.001	10.2	=0.013
	L	4.5	=0.067	2.9	=0.128	1.7	=0.223
	T×L	7.6	=0.024	18.3	=0.003	7.8	=0.023
Carbo	T	941.5	<0.001	73.1	<0.001	316.3	<0.001
	L	4773.8	<0.001	262.8	<0.001	1896.6	<0.001
	T×L	370.3	<0.001	26.5	=0.001	105.7	<0.001
Lipid	T	333.3	<0.001	359.6	<0.001	71.7	<0.001

https://doi.org/10.5194/egusphere-2025-5131
Preprint. Discussion started: 18 November 2025

	L	1281.1	<0.001	377.7	<0.001	128.6	<0.001
	T×L	32.1	<0.001	62.3	<0.001	4.6	=0.065

https://doi.org/10.5194/egusphere-2025-5131
Preprint. Discussion started: 18 November 2025

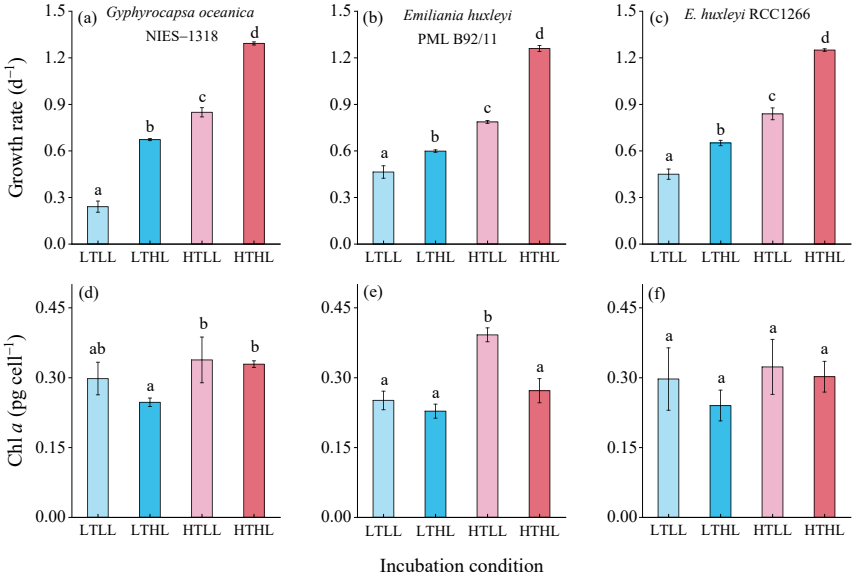

Figure 1

https://doi.org/10.5194/egusphere-2025-5131
Preprint. Discussion started: 18 November 2025

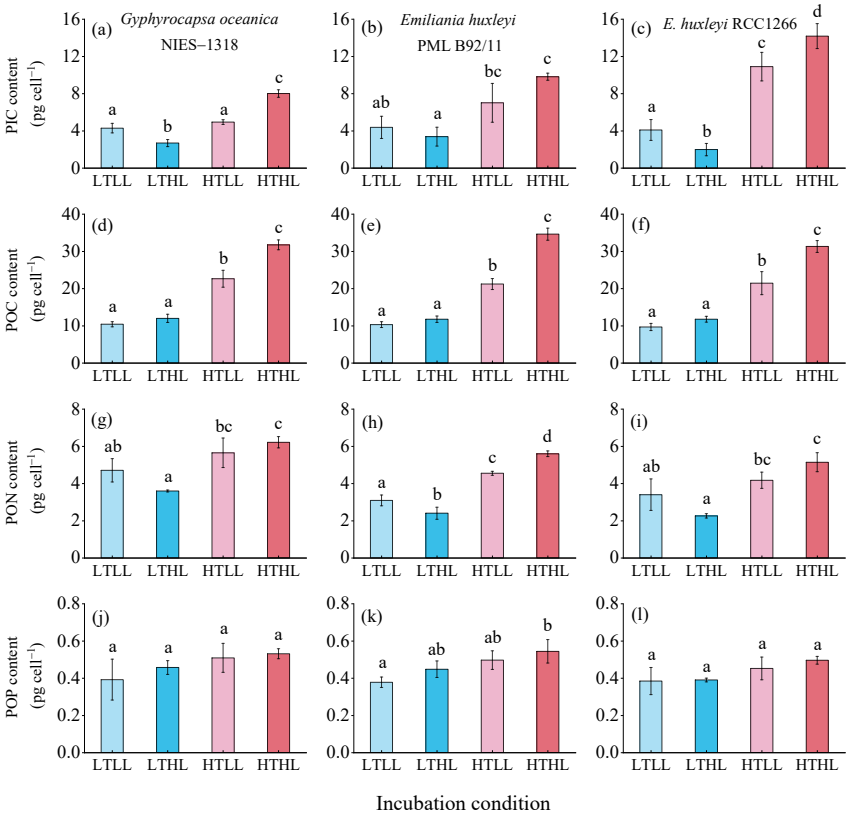

Figure 2

https://doi.org/10.5194/egusphere-2025-5131
Preprint. Discussion started: 18 November 2025

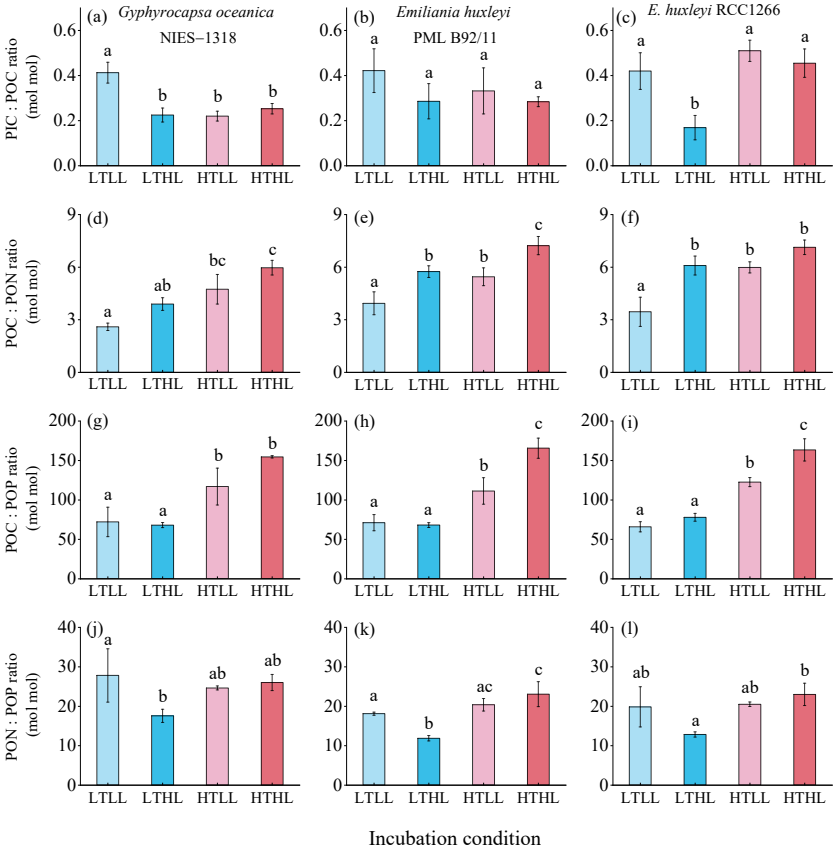

Figure 3

https://doi.org/10.5194/egusphere-2025-5131
Preprint. Discussion started: 18 November 2025

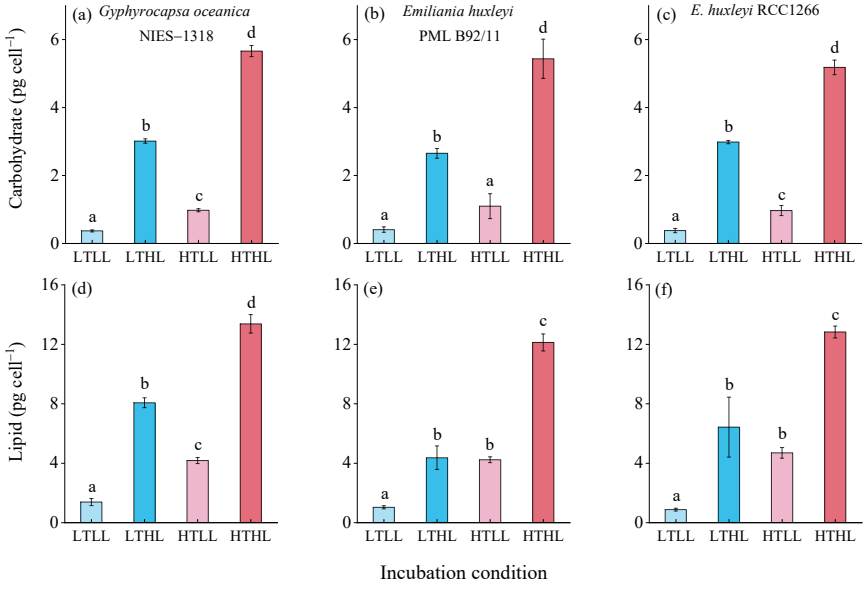

Figure 4